JOURNAL OF SOLID STATE CHEMISTRY 75, 296–304 (1988)

The Structures of the η-Carbides Ni_6Mo_6C, Co_6Mo_6C, and $Co_6Mo_6C_2$

J. M. NEWSAM, A. J. JACOBSON, L. E. McCANDLISH, AND R. S. POLIZZOTTI

Exxon Research and Engineering Company, Route 22 East, Annandale, New Jersey 08801

Received August 3, 1987, in revised form February 8, 1988

The structures of the three η-carbides Ni_6Mo_6C, Co_6Mo_6C, and $Co_6Mo_6C_2$, prepared by a new synthetic route, have been determined by Rietveld analyses of monochromatic neutron powder diffraction data. All three materials share the η-carbide structure-type with space group $Fd\bar{3}m$ (No. 227) and a = 10.8932(3) Å, a = 10.8998(2) Å, and a = 11.0709(3) Å, respectively. In the η-12 carbides, Ni_6Mo_6C and Co_6Mo_6C, the carbon atoms are exclusively located on the 0 0 0 (8a) sites, the 1/8 1/8 1/8 (16c) sites being vacant. In the η-6 carbide, $Co_6Mo_6C_2$, on the other hand the 16c sites are completely filled while the 8a sites are vacant. These studies both demonstrate that the compound precursor synthesis route used here yields high-quality, homogeneous materials and provide precise structural details for the η-12 and η-6 carbide phases. The differences between these two structures are discussed. The complete absence of solid solubility between the η-12 and η-6 phases is considered to reflect the limited separation of only 2.4 Å between the 8a and 16c carbon atom sites. The Mo : Co ratio of the η-6 phase is observed to be slightly greater than 1.0, with a refined formula $Co_{5.87(2)}Mo_{6.13(2)}C_2$, reflecting partial Mo occupancy of the Co2(16d) site. Overall sample stoichiometry (Mo : Co = 1.00) is maintained by the presence of Co_3Mo.

Introduction

The ternary phase diagrams for the M^{I} (M^{I} = Fe, Ni, or Co)–M^{II} (M^{II} = Mo or W)–C systems exhibit a wealth of discrete phases (*1*). The η-carbides, $M^{I}_6M^{II}_6C_n$, n = 1 (η-12), 2 (η-6), or 3 (η-4), in common with other interstitial transition metal carbides (*2*) are very hard and have high melting points. (In our notation an η–n phase has a metal to carbon atom ratio of n.) Structural data on carbides (and nitrides) based on T_6X (X = C or N) octahedra were summarized in 1965 by Parthe *et al.* (*3*). The η-carbides can be described by the general formula $M^{f}_6M^{d}_2M^{e}_4X^{c}_nX^{a}_m$ where ($M^{f} \equiv$ Mo, W; M^{d} = Mo, W, Fe, Co, Ni; M^{e} = Fe, Co, Ni; and n, m = 2, 1; 2, 0; or 0, 1. The superscript letters are those of the Wyckoff notation for the respective crystallographic sites—see below). The structures of the η-carbides are of the $E9_3$ (or filled Ti_2Ni) type and adopt space group symmetry $Fd\bar{3}m$ (No. 227). The origin is by convention chosen at the position of point symmetry $\bar{4}3m$. The metal atoms M^{f}, M^{d}, and M^{e} adopt the special positions x 0 0 (48f) with $x \simeq 0.19$, 5/8 5/8 5/8 (16d), and x x x (32e) with $x \simeq 0.83$. The interstitial species, X, occupy the octahedrally coordinated sites 0 0 0 (X^{a} – 8a) and/or 1/8 1/8 1/8 (X^{c} – 16c). Complete filling of one or both of these interstitial sites gives rise to three possible limiting compositions. For both sites filled (n = 2, m = 1), the metal to carbon atom ratio is 4, the phases being termed η-4. $Nb_8Zn_4C_3$ is

0022-4596/88 $3.00

apparently an example of an η-4 carbide phase (*4*). The η-6 and η-12 phases have, respectively, completely filled 16c ($n = 2$, $m = 0$) or 8a sites ($n = 0$, $m = 1$).

The compositions observed for the η-carbide phases are consistent with carbon atom occupancy of these interstitial octahedral sites, although direct diffraction evidence is limited. The relatively low scattering power of carbon makes its location in the presence of elements of much larger atomic number difficult in a powder X-ray diffraction (PXD) experiment. Powder neutron diffraction (PND) measurements which provide much better sensitivity to the carbon atom parameters are therefore preferred. Powder diffraction studies of the η-4 phase $Nb_8Zn_4C_3$ (PXD) (*4*), the η-6 phases W_4Co_2C (PXD) (*5, 6*) and W_3Fe_3C (PXD) (*7, 8*), and the η-12 phase W_6Fe_6C (PND) (*9*) have been reported (see (*3*)). The oxygen-stabilized phases $Zr_3V_3OD_x$ that share the η-carbide structure have also been studied by PND (*10*). A PND study of the different but related Nowotny phase $Mo_{4.8}Si_3C_{0.6}$ (*3*) confirmed carbon atom occupancy of the octahedral interstices in the structure.

The conventional synthetic route to the η-carbide phases involves arc-melting combinations of the elements, remelting, and extensive annealing (*1*). McCandlish and Polizzotti (*11*) have recently described a new route to the η-phases $Ni_6Mo_6C_n$ and $Co_6Mo_6C_n$, $n = 1$ and 2, that involves intimate mixing of the metal components via a molecular precursor. In the present report we describe the determination of the structures of three of these phases, Ni_6Mo_6C, Co_6Mo_6C, and $Co_6Mo_6C_2$, by Rietveld analyses of powder neutron diffraction data.

Experimental

Synthesis of the η-Carbide Phases

The η-carbide phases were produced by two-stage reaction of the nickel or cobalt trisethylenediamine molybdates, $M(en)_3MoO_4$, using methods described earlier (*11*). The molybdate salts were first heated from 25°C to 650°C in a flowing mixture of He and H_2 to produce precursors of intermediate structures in which the transition metal atoms presumably remain intimately mixed on an atomic level. These precursor materials were subsequently converted to the desired products by reaction at 1000°C in flowing CO/CO_2 gas mixtures of appropriate carbon activities. The intimate mixing of the metal components in the precursor circumvents the kinetic barrier (to the formation of the thermodynamically most-stable product) that can be problematic in the conventional synthesis procedures. Chemical precursors have been used in the synthesis of a range of refractory mixed-transition metal oxides (*12–14*). The specific details of the syntheses of Ni_6Mo_6C, Co_6Mo_6C, and $Co_6Mo_6C_2$ were given earlier (*11*). The procedures have excellent reproducibility and to produce sufficient material for the powder neutron diffraction experiments a series of 2 g lots of each material was prepared using identical conditions. The separate lots were then combined to yield approximately 10 g of each η-carbide phase. PXD scans of both η-12 materials showed only lines that could be indexed on the basis of face-centered cubic unit cells with the least-squares optimized lattice constants given in Table 1. Silicon was used as an internal standard. A detailed examination of the PXD pattern of the η-6 material, $Co_6Mo_6C_2$, revealed traces of a second phase, Co_3Mo (see below).

Powder Neutron Diffraction Measurements

Approximately 5 g of each material was loaded into a 7/16-in. inside diameter, 0.005-in. walled vanadium can with aluminum end caps. The powder neutron diffraction data were collected at ambient temperature (298(5) K) on the powder diffractometer

TABLE I

FINAL OVERALL PARAMETERS WITH ESTIMATED STANDARD DEVIATIONS IN PARENTHESES

	Ni_6Mo_6C	Co_6Mo_6C	$Co_6Mo_6C_2$
a Å (PXD)[a]	10.8911(3)	10.9021(3)	11.0720(3)
a Å (PND)	10.8932(3)	10.8998(2)	11.0709(3)
Volume Å^3	1292.6(1)	1294.9(1)	1356.9(1)
a (Aluminum) Å	—	4.065(1)	4.057(1)
Half-width parameters[b] (deg^2)			
U	0.84(2)	0.87(2)	0.93(3)
V	−0.77(3)	−0.81(3)	−0.83(3)
W	0.36(1)	0.46(1)	0.44(1)
Zero point error (deg)	−0.143(2)	−0.033(2)	−0.019(2)
Asymmetry parameter	0.23(3)	0.16(2)	0.17(1)
γ	0.245(7)	0.237(8)	0.229(8)
Number of data points	1010	1010	1010
Number of contributing reflections	84	84[9][c]	85[9]
Number of atomic variables	8	8	9
Total number of variables	16	18	19
R_B (reflection intensity)	2.04	1.43[1.39]	1.40[1.38]
R_p (profile)	3.27	1.95	2.29
R_{wp} (weighted profile)	4.30	2.57	2.94
R_e (expected)	1.71	1.37	1.53

[a] Least-squares optimized lattice constants based on reflection positions derived in automatic peak searches of Siemens D500 diffractometer data.

[b] The definitions of the half-width parameters, the asymmetry parameter, the Lorentzian–Gaussian mixing parameter, γ, and the various residuals are given in (*16*) and (*17*).

[c] Figures in square brackets refer to the minority aluminum component.

equipped with a linear position sensitive detector at the Missouri University Research Reactor (*15*). The diffraction profiles $5.0 \leq 2\theta \leq 105.0°$ were each accumulated over a total of some 22 hr at four settings of the detector using a mean incident neutron wavelength of 1.2891 Å selected from the (220) planes of a Cu monochromator at a take-off angle of 60.6°. The wavelength was calibrated using the least-squares optimized lattice constants of the three carbide phases determined from the powder X-ray data (Table I). The full matrix Rietveld refinements (*16*) were achieved using a locally modified version of Wiles and Young's (*17*) DBW3.2 program implemented on a VAX 11/750 computer system. Scattering lengths of 10.30, 6.95, 6.648, and 2.53 fm ($\times 10^{-15}$ m) for Ni, Mo, C, and Co, respectively, were taken from Koester *et al.* (*18*).

Structure Refinements

Ni_6Mo_6C. The powder neutron diffraction profile of the η-12 phase Ni_6Mo_6C calculated using atomic coordinates in space group $Fd\bar{3}m$ (No. 227) taken from the work of Leciejewicz (*9*) gave poor agreement with that observed as a result of a (typographical) error in the x coordinate of W1. Interactive modeling of the Fe_6W_6C structure indicated the correct value of this parameter to be approximately −0.07, the inverse of the published value of 0.071. Using the corrected value, the calculated

TABLE II

FINAL ATOMIC PARAMETERS FOR THE η-CARBIDE PHASES WITH ESTIMATED STANDARD DEVIATIONS IN PARENTHESES

Atom	Site	Population[a]	x	y	z	B (Å^2)
			Ni_6Mo_6C			
Ni1	32e	4.0	0.8333(1)	x	x	0.33(2)
Ni2	16d	2.0	0.625	0.625	0.625	0.35(2)
Mo1	48f	6.0	0.1970(1)	0.0	0.0	0.45(2)
C1	8a	1.03(1)	0.0	0.0	0.0	0.40(7)
C2	16c	−0.03(1)	0.125	0.125	0.125	"
			Co_6Mo_6C			
Co1	32e	4.0	0.8326(1)	x	x	0.41(4)
Co2	16d	2.0	0.625	0.625	0.625	0.38(6)
Mo1	48f	6.0	0.1969(1)	0.0	0.0	0.40(1)
C1	8a	1.012(8)	0.0	0.0	0.0	0.26(5)
C2	16c	−0.003(7)	0.125	0.125	0.125	"
			$Co_6Mo_6C_2$			
Co1	32e	4.0	0.8319(1)	x	x	0.36(4)
Co2	16d	2.22(3)[b]	0.625	0.625	0.625	0.48(8)
Mo1	48f	6.0	0.1985(1)	0.0	0.0	0.44(1)
C1	8a	0.008(5)	0.0	0.0	0.0	0.35(3)
C2	16c	2.03(1)	0.125	0.125	0.125	"

[a] Population parameters, P, are expressed in terms of the formula $M_6Mo_6C_n$. Conventional site occupancy factors can be calculated as $8 \times P$ divided by the respective site multiplicities given in column 2.

[b] When the Co2 occupancy was fixed at 2.0, the residuals were significantly worse and the temperature factor for Co2 was unacceptably low (B = 0.04(6)). The difference in the site occupancy from 2.0 reflects partial occupancy of the Co2 site by Mo (see text).

diffraction profile immediately gave reasonable agreement with that observed. The Rietveld refinements then converged smoothly to the parameters given in Tables I and II. The refinements indicated the C1 (8a) site to be fully occupied. The C2 (16c) site, on the other hand, was found to be vacant. The occupancy of this site was included as a variable in the final refinements (Table II) to indicate the precision with which the present analysis describes the complete partitioning of the carbon atoms on the 8a sites. The final observed and calculated profiles are shown in Fig. 1. Selected separations and angles are listed in Tables III and IV.

Co_6Mo_6C and $Co_6Mo_6C_2$. The results of the Ni_6Mo_6C structure analysis were used as starting values for refinement of the structures of the η-12 phase, Co_6Mo_6C, and the η-6 phase, $Co_6Mo_6C_2$. Small contributions from the aluminum end caps of the sample cans were observed in the diffraction profiles of both materials. The relative scale factor and unit cell constant of the aluminum component were therefore included in final biphasic refinements. For the η-6 phase, $Co_6Mo_6C_2$, the occupancies of the Co[e], Co[d], and Mo[f] metal atom sites were initially constrained to those expected on the basis of this ideal composition. The temperature factor of the M^d or Co2 site, however, converged to an unrealistically low value (Table II footnote). When al-

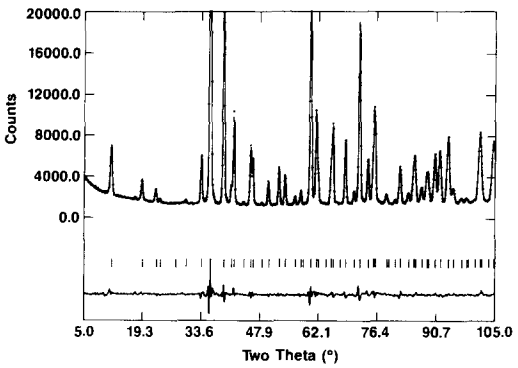

FIG. 1. Final observed (●), calculated (continuous line connecting computed data points), and difference (lower same scale) powder neutron diffraction profiles for the η-12 phase Ni_6Mo_6C. The positions of the contributing reflections are indicated by the vertical bars. The background has not been subtracted from the data and the calculated profile at each point includes an estimated background derived by linear interpolation between the small set of input values. The maximum observed count is 54,500.

TABLE III

SEPARATIONS (Å) WITH ESTIMATED STANDARD DEVIATIONS IN PARENTHESES

	Ni_6Mo_6C	Co_6Mo_6C	$Co_6Mo_6C_2$
$M1^a$–$^{51}M1^b$	2.565(1)	2.546(3)	2.565(3)
–$^{51}M2$	2.358(1)	2.355(1)	2.388(1)
–^{50}Mo1	2.590(1)	2.601(1)	2.653(1)
–^{67}Mo1	2.715(1)	2.719(2)	2.749(2)
$M2$–^{2}Mo1	2.732(1)	2.735(1)	2.766(1)
Mo1–^{14}Mo1	2.843(1)	2.845(1)	2.883(1)
–^{5}Mo1	3.036(2)	3.036(1)	3.107(1)
$M1$–C1	3.146(1)	3.161(1)	[3.223(1)]^c
–C2	[3.242(1)]	[3.254(1)]	3.314(1)
Mo1–C1	2.146(1)	2.147(1)	[2.197(1)]
–C2	[2.079(1)]	[2.080(1)]	2.119(1)
[C1–C2	2.358	2.360	2.397]

^{a} M = Ni or Co; $M1$, $M2$, and Mo1 occupy the 32e, 16d, and 48f sites, respectively.

^{b} The superscript number preceding each atom label (where absent read 1) is the number of the symmetry operator that has been applied (*22*). For numbers N, $48 < N < 97$, the centering operation (0, 1/2, 1/2) has also been applied.

^{c} The square brackets indicate distances to sites that are not occupied in the material in question.

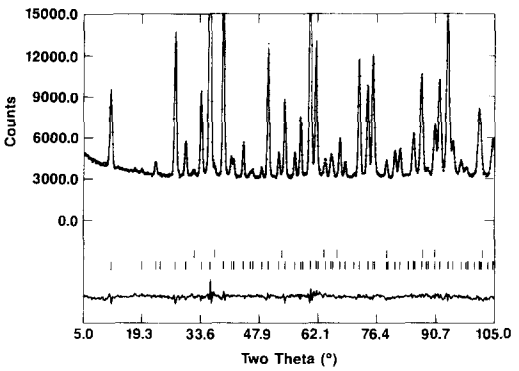

FIG. 2. Final observed, calculated, and difference profiles for the η-12 phase Co_6Mo_6C (legend as for Fig. 1). The upper and lower reflection bars indicate the positions of the contributing reflections from the η-12 phase (lower) and from the minor aluminum component (upper). The maximum observed count is 38,200.

lowed to vary, the residuals were significantly improved and the occupancy converged to 2.22(3). This value apparently indicates 6.3% occupancy of the M^d, Co2 site by molybdenum (see below). The final parameters for the Co_6Mo_6C and Co_6Mo_6C phases are given in Tables I and II. The corresponding observed and calculated profiles are displayed in Figs. 2 and 3. Selected separations and angles are given in Tables III and IV.

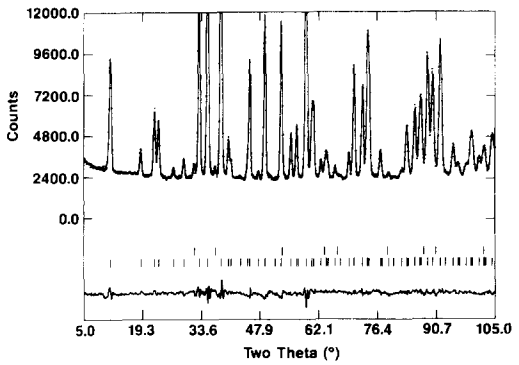

FIG. 3. Final observed, calculated, and difference profiles for the η-6 phase $Co_6Mo_6C_2$ (legend as for Figs. 2 and 1). The maximum observed count is 24,600.

TABLE IV

SELECTED ANGLES (°) WITH ESTIMATED STANDARD DEVIATIONS IN PARENTHESES[a]

	Ni_6Mo_6C	Co_6Mo_6C	$Co_6Mo_6C_2$
Angles about Mo1			
^{9}Mo1–^{2}Mo1–^{22}Mo1	106.68(4)	106.71(2)	106.25(2)
–^{14}Mo1	57.73(3)	57.76(1)	57.39(2)
–^{31}Mo1	145.17(2)	145.18(1)	144.96(1)
^{14}Mo1–^{1}Mo1–^{22}Mo1	110.34(3)	110.37(2)	109.93(2)
Angles about C2[b]			
$^{50}M1$–^{1}C2–$^{63}M1$	75.21(1)	75.03(3)	74.87(3)
–^{1}Mo1	52.92(1)	52.98(3)	53.09(2)
–^{24}Mo1	56.39(4)	56.26(3)	55.69(3)
–^{9}Mo1	123.61(4)	123.74(3)	124.31(3)
–^{14}Mo1	127.08(1)	127.02(3)	126.91(2)
–^{1}C1	66.17(1)	66.33(2)	66.48(2)
^{1}Mo1–^{1}C2–^{9}Mo1	93.75(5)	93.71(2)	94.29(3)
–^{14}Mo1	86.25(5)	86.29(2)	85.71(3)
–^{1}C1	57.44(3)	57.41(2)	57.83(2)

[a] Atom lettering follows the same convention as Table III.

[b] Comparable angles about C1 (that are fixed by symmetry) are $^{1}M1$–^{1}C1–^{1}Mo1 125.26°, $^{1}M1$–^{1}C1–^{50}Mo1 54.74°, and $^{1}M1$–^{1}C1–^{50}C2 70.53°.

Results and Discussion

The structures of the η-carbides are complicated and somewhat difficult to visualize (see Figs. 4–6). The structure is based on that of diamond. A M_6^f octahedron is centered on each 8a interstitial carbon atom site, these sites coinciding with the lattice points of the diamond structure. Four additional M_6^f octahedra, arranged tetrahedrally, are joined to this central octahedron in a face-shared manner. The second set of interstitial carbon atom sites, 16c, occurs at the centers of these four additional octahedra. This combined M_6^f unit defines one of the two interpenetrating metal substructures, that adopted by Mo in the phases discussed here (Fig. 4). The second metal substructure consists of M_4^e tetrahedra centered on the 1/2 1/2 1/2 (8b) sites which define a second diamond lattice (that is displaced from the first by 1/2 1/2 1/2). The four faces of these tetrahedra are capped by the M^d metal atoms which are shared between adjacent M_4^e tetrahedra. This combination of M_4^e tetrahedra and capping M^d species thus form *stellae quadrangula* (*19*) (Fig. 5). The two interpenetrating (and bonded) metal atom substructures (Fig. 6) have been viewed in terms of the periodic minimal surfaces (*20*).

The agreements between the final calculated PND profiles and those observed are

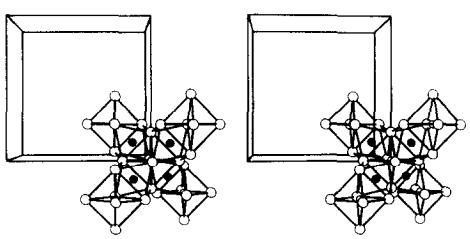

FIG. 4. Stereoview of a portion of the Mo^f, C^a, C^c (filled circles, site not populated in the η-12 phase) substructure of the η-12 phase Ni_6Mo_6C.

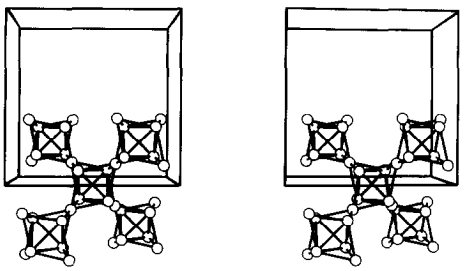

FIG. 5. Stereoview of a portion of the Ni^e (central tetrahedra) and Ni^d (capping atoms) substructure of the η-12 phase Ni_6Mo_6C.

excellent (Figs. 1–3), demonstrating graphically that the molecular precursor route yields high-quality materials with excellent homogeneity. The present results provide the most precise data available to date on the structures of η-carbide phases. The two η-12 phases Ni_6Mo_6C and Co_6Mo_6C are similar (Tables I–IV) indicating that the change in the M^d and M^e species has only subtle effects on the structure. Comparing the η-12 and η-6 phases in the Co–Mo system, however, shows that the increased carbon atom population results in a lengthening of all metal–metal bonds and a corresponding increase in the cubic unit cell edge.

The present results provide insight into the structural basis for the observed phase diagrams (*1*). The conventional synthetic procedures used by Fraker and Stadelmeier (*1*) to define the 1000°C isothermal phase diagram (arc melting, remelting, annealing at 1250°C for 20 hr and, finally, annealing at 1000 ± 10°C for 150 hr) could potentially permit phases stable in the melt to persist as metastable phases in the solid after these moderate annealing conditions. The new synthesis route (*11*) affords the equilibrium phases directly, and the observed phase behavior is consistent with the earlier results (*1*). The Co/Mo composition range for pure η-6 phases, for example, extends from approximately 24.5% Co ($\equiv Co_{2.94}Mo_{9.06}$) to 45.5% Co ($\equiv Co_{5.45}Mo_{6.54}$) (*1*). The composition derived from the present diffraction results for the η-6 phase, $Co_{5.87(2)}Mo_{6.13(2)}C_2$ (Table II), is slightly more cobalt-rich than this upper limit, but still less than the ideal ratio 1 : 1. The manner in which the Co : Mo compositional variability is accommodated in the η-carbide structure is found to be molybdenum substitution at the M^d, Co2 site, consistent with the earlier PXD results of Kiessling (*6*) for the similar phase W_4Co_2C.

The published phase diagram indicates that the range of Co–Mo compositions over which the η-6 phase forms occurs at a constant atomic percentage of carbon (*1*). This range of Co : Mo compositions reflects varying Co : Mo (or Co : W (*6*)) population of the M^d sites that comprise the stellae quadrangula. The composition of the first coordination shell of the interstitital carbon atoms (the M_6^f octahedra) is invariant. Interestingly, in the Ni–Mo system the carbon content of the η-6 phase apparently varies with Ni : Mo ratio (*1*). This suggests that the compositional variability may be accommodated by a different metal atom distribution, possibly involving the M^f sites. The structures of these Ni–Mo η-6 phases will thus be of some interest.

In the present syntheses the starting materials had Co : Mo (Ni : Mo) ratios of 1.000, as confirmed by the structure results for the η-12 phases. The slight molybdenum excess in the η-6 phase thus implies the presence of a second, molybdenum-poor

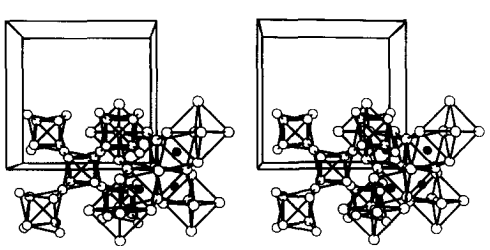

FIG. 6. Stereoview showing the Ni^e, Ni^d, and Mo^f substructures combined.

phase. An extended scan of the PXD profile revealed weak peaks at d = 2.223 Å and d = 2.065 Å, with approximately equal peak intensities of 0.2% that of the adjacent 333/115 peak of the η-6 phase. These are indexed as the 200 and 002 reflections from Co_3Mo (described as hexagonal, $P6_3/mmc$; a = 5.13 Å, c = 4.11 Å (*21*)). No significant intensity was observed at d = 1.901 Å, the position of the most intense peak (101) in the PXD pattern of α-Co.

The η-6 and η-12 phases show no solid solubility. That is, in the Co–Mo and Ni–Mo systems the 8a and the 16c interstitial carbon atom sites are not occupied simultaneously. This is not unexpected in light of the limited separation of ~2.4 Å (Table III) between these two positions which might be expected to make joint occupancy energetically unfavorable. In the Nb–Zn system, however, the η-4 phase, $Nb_8Zn_4C_3$, has been observed (*4*) in which both 8a and 16c sites are apparently fully occupied.

The phase diagrams and structures of the η-carbide materials thus continue to pose several interesting questions, particularly with respect to their stability fields and local electronic structures. For example, the Co–Mo or Ni–Mo composition ranges over which the η-12 phases form are limited. Inspection (for example in terms of electron count) of the combinations of elements that form these phases does not provide immediate insight into these questions. It is, therefore, likely that an adequate rationalization of the observed compositional fields and chemical properties will be provided only by detailed band structure calculations. It will also be interesting to examine the interaction of these materials with hydrogen. Structural studies of the $Zr_3V_3OD_x$ system (*10*) that shares the η-carbide structure-type demonstrate that several interstitial sites (coordinated by Zr and V) can be occupied by hydrogen, suggesting that hydrogen population of similar interstitial sites may be possible also in the Co–Mo and Ni–Mo η-carbide structures.

Acknowledgments

We thank J. C. Scanlon for help with the PXD analyses and W. B. Yelon for accumulating the PND data.

References

1. A. C. Fraker and H. H. Stadelmaier, *Trans. Metall. Soc. AIME* **245,** 847–850 (1969).
2. L. K. Storms, "The Refractory Carbides," Academic Press, New York/London (1967).
3. E. Parthe, W. Jeitschko, and V. Sadagopan, *Acta Crystallogr.* **19,** 1031–1037 (1965).
4. W. Jeitschko, H. Holleck, H. Nowotny, and F. Benesovsky, *Monatsh. Chem.* **95,** 1004–1006 (1964).
5. E. N. Kislakova, *J. Phys. Chem. USSR* **17,** 10 (1943).
6. R. Kiessling, *in* "Proceedings, International Symposium on the Reactivity of Solids, Gothenburg," pp. 1065–1068 (1965).
7. A. Westgren, *Jernkontorets Ann.* **116,** 1–14 (1933).
8. M. H. Mueller and H. W. Knott, *Trans. Metall. Soc. AIME* **227,** 674–678 (1963).
9. J. Leciejewicz, *J. Less-Common Met.* **7,** 318–320 (1964).
10. F. J. Rotella, H. E. Flotow, D. M. Gruen, and J. D. Jorgensen, *J. Chem. Phys.* **79,** 4522–4531 (1983).
11. L. E. McCandlish and R. S. Polizzotti, U.S. Patent application filed May 22 (1987).
12. H. S. Horowitz and J. M. Longo, *Mater. Res. Bull.* **13,** 1359 (1978).
13. J. M. Longo and H. S. Horowitz, *in* "Preparation and Characterization of Materials" (J. M. Honig and C. N. R. Rao, Eds.), Academic Press, New York (1981).
14. C. N. R. Rao, J. Gopalkrishnan, K. Vidyasagar, A. K. Ganguli, A. Ramanan, and L. Ganapathi, *J. Mater. Res.* **1,** 280–294 (1986).
15. C. W. Tompson, D. F. R. Mildner, M. Mehregany, J. Sudol, R. Berliner, and W. B. Yelon, *J. Appl. Crystallogr.* **17,** 385–394 (1984).
16. H. M. Rietveld, *J. Appl. Crystallogr.* **2,** 65–72 (1969).
17. D. B. Wiles and R. A. Young, *J. Appl. Crystallogr.* **14,** 149–151 (1981).

18. L. KOESTER, H. RAUCH, M. HERKENS, AND K. SCHRÖDER, K. F. A. Report (K. F. A. Jülich) Jül-1755 (1981).
19. H. NYMAN, S. ANDERSON, B. G. HYDE, AND M. O'KEEFFE, *J. Solid State Chem.* **26,** 123–131 (1978).
20. S. ANDERSON, S. T. HYDE, AND H. G. SCHNERING, *Z. Kristallogr.* **168,** 1–17 (1984).
21. L. ALTE DA VEIGA, *Acta Crystallogr.* **28,** 855–857 (1965).
22. "International Tables for Crystallography," Vol. A, p. 687, Reidel, Dodrecht (1983).